Polymorphism of Oriented Syndiotactic Polypropylene

Liberata Guadagno, Concetta D'Aniello, Carlo Naddeo, and Vittoria Vittoria*

Dipartimento di Ingegneria Chimica e Alimentare, Università di Salerno, Via Ponte Don Melillo, 84084 Fisciano (Sa), Italy

Received April 4, 2000; Revised Manuscript Received May 22, 2000

ABSTRACT: Two syndiotactic polypropylene (sPP) samples were obtained by quenching the melt in a bath at 0 °C, for 1 min (sample **1A**) and 3 days (sample **1B**). In these conditions sample **1A** crystallized in the disordered form I, having the chains in helical conformation, whereas sample **1B** formed a mesophase with the chains in trans-planar conformation, as evident by X-rays and FTIR analysis. Samples **1A** and **1B** were drawn at room temperature, obtaining fibers with a draw ratio between 4 and 7, which were analyzed under tension. The fibers, with a draw ratio 4 and 5, obtained from sample **1A**, show a well oriented helical form and a fraction of oriented trans-planar form. When the draw ratio reaches the value of 6 and 7, the crystalline form III with chains in trans-planar conformation is obtained. At variance, the fibers obtained from sample **1B** show a progressive orientation of the trans-planar mesophase, and the appearance of form III at draw ratio of 6 and 7. Therefore, the fibers drawn at $\lambda = 6$ and 7, coming from the two samples **1A** and **1B**, are very similar, as shown by X-rays and FTIR analysis. Despite this similarity, upon releasing the tension, they undergo different transformations, going toward the oriented helical form or the oriented trans-planar mesophase, respectively.

Introduction

The recent use of metallocene catalysts for producing polypropylenes with new tacticity microstructures and high molecular weights spurred many investigations, with the purpose to explore new properties, beyond those of conventional isotactic polypropylene. In particular, syndiotactic chains with a wide range of tacticities and molecular weights were obtained and investigated.[1−3] Although the syndiotactic polypropylene displays interesting properties, it shows a poorer behavior than the isotactic one: the slow crystallization rate and a very complicated polymorphism, not yet fully clarified, are some examples.[4−20]

Four crystalline forms of sPP have been described so far. Forms I and II are characterized by chains in $(T_2G_2)_n$ helical conformation,[4,10] whereas forms III and IV present chains in *trans*-planar and $(T_6G_2T_2G_2)_n$ conformations,[8−9] respectively. Form I is the stable form of sPP obtained under the most common conditions of crystallization either from the melt state or from solution as single crystals.[4−7,13] In this form, the helical chains are packed, in the limit-ordered structure, with an alternation of right-handed and left-handed helices along both axes of the unit cell, that is othorhombic with axes $a = 14.50$ Å, $b = 11.20$ Å, and $c = 7.45$ Å. Disorder in this regular alternation is present in samples crystallized from the melt at low temperatures: in this case the unit cell is orthorhombic with axes $a = 14.50$ Å, $b = 5.60$ Å, and $c = 7.45$ Å.

Form II corresponds to the C-centered structure in which the helical chains have the same chirality. So far, form II was obtained by stretching at room-temperature compression molded specimens of sPP samples with low stereoregularity.[4,10] Stretching the most stereoregular samples, obtained with the new metallocenic catalysts, fibers in the trans-planar form III are obtained.[14] However, also in this case, the pure form II may be obtained upon release of the tension in fibers initially in the trans-planar form III. Under these conditions, a phase transition from form III to the isochiral form II occurs. Annealing fibers samples of form II or form III at temperatures higher than 100 °C gives mixtures of oriented form I and II.[10] The trans-planar form III is the metastable polymorph of sPP. It is obtained through cold drawing of sPP samples, quenched from melt at low temperatures.[8] Recently, Nakaoki et al.[20] reported the spontaneous crystallization of the trans-planar form III, taking the sPP, after melting, in a bath at 0 °C for a long time. At variance, we suggested that this new phase, characterized by chains in trans-planar conformation, does not correspond to the crystalline form III and should be identified as a mesophase, or also paracrystalline, disordered phase, containing lateral disorder in the packing of the trans-planar chains. This phase, stable up to 80 °C, is almost completely transformed into the more stable form I at higher temperatures.[21]

In this paper we investigated the drawing at room temperature of this new phase, and compared it to the drawing of a sample in form I, to obtain new information on the complex polymorphic behavior of sPP. We investigated the influence of the initial structure on the structure of the fibers, both before and after the release of the tension, trying to understand the dependence of the final structure on the initial one, for fibers both under tension and released. In fact it was observed that sPP fibers undergo a strong shrinkage when the tension is relieved, much higher that the shrinkage of isotactic polypropylene fibers.[22,23]

Experimental Section

The syndiotactic polypropylene was synthesized according to a previous procedure.[24] The polymer was analyzed by ^{13}C NMR spectroscopy at 120 °C on an AM 250 Bruker spectrometer operating in the FT mode at 62.89 MHz, by dissolving 30 mg of sample in 0.5 mL of $C_2D_2Cl_4$. Hexamethyldisiloxane was used as internal chemical shift reference. It resulted composed of 91% syndotactic pentads.

The sPP powders were molded in a hot press, at 150 °C, forming a film 0.1 mm thick, and rapidly quenched at 0 °C in an ice−water bath. One sample was extracted from the bath after 1 min (sample **1A**). Another sample was kept in the cold bath for 3 days (sample **1B**).

10.1021/ma0005973 CCC: $19.00
Published on Web 07/22/2000

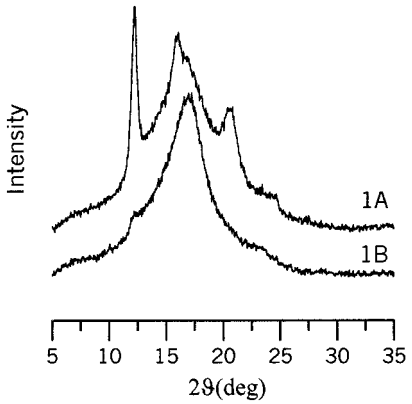

Figure 1. X-ray powder diffractograms of sample **1A** and sample **1B**.

Sample **1A** and sample **1B** were drawn up to $\lambda = 4$, 5, 6, and 7 (**2A**, **3A**, **4A**, **5A**, and **2B**, **3B**, **4B**, **5B**), at room temperature, using a dynamometric apparatus INSTRON 4301. The deformation rate was 10 mm/min, and the initial length of the sample was 10 mm. The drawn samples were analyzed by X-rays and FTIR, under tension, before unhooking. Samples **4A** and **4B** were unhooked (**1C** and **2C**) and again analyzed.

Fiber diffraction spectra were recorded under vacuum by means of a cylindrical camera with a radius of 57.3 mm and the X-ray beam direction perpendicular to the fiber axis (V-filtered Cr Kα radiation). The imaging plate Fujix BAS-1800 system was used to record the diffraction patterns.

The infrared spectra were obtained in absorbance by using a FTIR−Bruker IFS66 spectrophotometer with a resolution of 4 cm^{-1} (32 scans collected). The absorbances of the trans-planar conformational bands at 831, 963, and 1132 cm^{-1} were normalized with the absorbance of the band at 1153 cm^{-1}. Since this band overlaps with other vibrational modes, it was decomposed in the different components, using a complex fitting in which a Lorentzian and a Gaussian contribution was considered in the form:

$$f(x) = (1 - L)H \exp - \left[\left(\frac{x - x_0}{w}\right)^2 (4 \ln 2)\right] + L\frac{H}{4\left(\frac{x - x_0}{w}\right)^2 + 1}$$

where X_0 is the peak position, H is the height, w is the width at half-height, and L is the Lorentzian component.

Results and Discussion

Powder Samples. The X-ray powder diffraction patterns of sample **1A** and sample **1B** are shown in Figure 1. The diffractogram of sample **1A** indicates that this sample crystallized in the usual form I, characterized by the most intense peaks at 12.3, 15.9, and 20.8° of 2ϑ. The absence of the (211) reflection at $2\vartheta = 18.9°$ indicates that we obtained a disordered modification of form I, as expected for a sample rapidly quenched to 0 °C. In this case, as well documented in other cases, departures from the fully antichiral packing both along *a* and *b* axes may occur, leading to a less ordered form. The preferential crystallization of this disordered form was always found in samples of low syndiotacticity, or in powder samples crystallized from the melt at low temperatures.[10]

The diffractogram of sample **1B**, kept at 0 °C for 3 days, shows a broad peak centered around $2\vartheta = 17°$, with a shoulder around $2\vartheta = 24°$. Nakaoki et al.[20] identified these reflections as characteristic of form III, having the chains in trans-planar conformation. At variance, we suggested that this new phase, stabilized at low temperature for a long time, although characterized by chains in trans-planar conformation, could not be identified as the known crystalline form III: it should be rather identified as a mesophase, or also paracrystalline, disordered phase, containing lateral disorder in the packing of the trans-planar chains.[21]

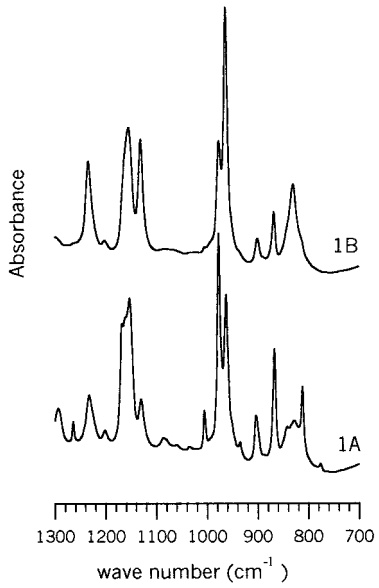

Figure 2. FTIR spectra in absorbance (1300−700 cm^{-1}) of sample **1A** and sample **1B**.

To confirm that samples **1A** and **1B** have the chains in different conformations, helical in sample **1A** and trans-planar in sample **1B**, in Figure 2 we report the FTIR spectra in absorbance (1300−700 cm^{-1}) of the two samples. Infrared analysis is very sensitive for the chain conformation determination: as matter of fact helical and trans-planar bands have been evidenced since the first preparation of the syndiotactic isomer of polypropylene.[25,26] We observe that, in sample **1A**, the bands of the helical form of sPP,[27] appearing at 810, 868, 977, and 1005 cm^{-1}, are very evident and well developed. At variance, in sample **1B**, the helical bands are absent, or strongly reduced, whereas the bands corresponding to long strands in trans-planar conformation, appearing at 831, 963, and 1132 cm^{-1} are very evident and well developed. This confirms that sample **1B**, kept in the cold bath for 3 days, assumed a prevalently trans-planar conformation. However, the presence of some helical bands, in particular the 868 and 977 cm^{-1} bands, indicates that a small fraction of chains in helical conformation was formed too, probably upon removing the sample from the cold bath. This is confirmed by a small trace, in the diffractogram of sample **1B** (see Figure 1), of the reflection at $2\vartheta = 12.3°$, corresponding to the (200) reflection of the helical form I.

On the other hand, in sample **1A**, the trans-planar bands at 831, 963, and 1132 cm^{-1}, are present too, although of reduced intensity respect to sample **1B**. This means that the permanence in the bath at 0 °C, even for 1 min, produced also in sample **1A** a small formation of a mesophase with chains in trans-planar conformation. This is also confirmed by the broadening of the (010) reflection at $2\vartheta = 15.9°$, with a prominent shoulder at $2\vartheta = 17°$, typical of the trans-planar mesophase (see Figure 1).

Therefore, quenching the sPP melt at 0 °C for 1 min allows the prevalent crystallization of form I, with the chains in helical conformation, crystallizing when the

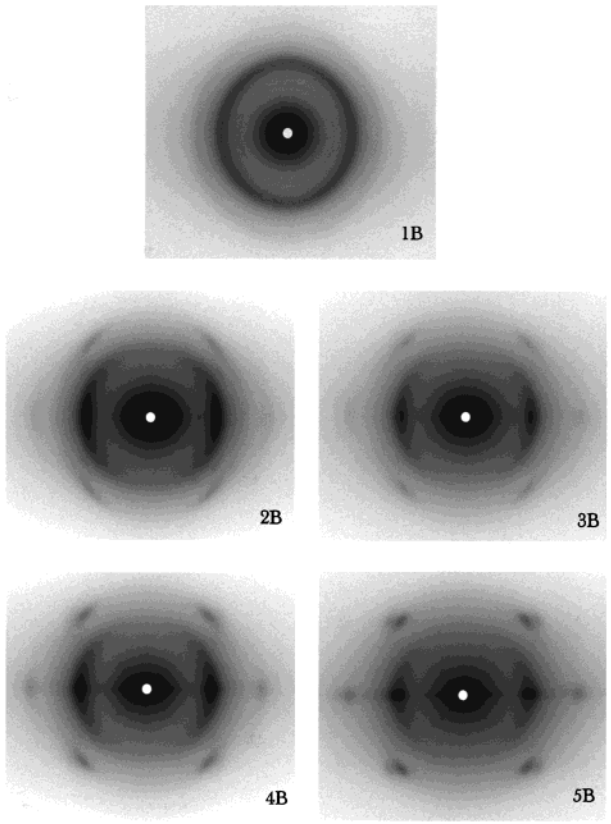

Figure 3. X-ray fiber diffraction patterns of the fibers with draw ratios $\lambda = 4$ (**2B**), $\lambda = 5$ (**3B**), $\lambda = 6$ (**4B**), and $\lambda = 7$ (**5B**), obtained from sample **1B**.

sample is extracted from the bath and brought at room temperature. A small quantity of mesophase with chains in trans-planar conformation was probably formed during the short time of permanence at 0 °C.

At variance, quenching the sPP melt at 0 °C and keeping it for 3 days at this temperature allows the prevalent formation of the trans-planar mesophase. A small amount of helical chains, probably formed when the sample is brought at room temperature, is present too.

Oriented Samples. Oriented fibers were obtained by stretching, at room temperature, the two sPP samples. Sample **1A** deforms with neck propagation, causing an extremely not homogeneous deformation, up to $\lambda = 4$. When the neck propagated to the whole sample, the deformation becomes homogeneous, and we observe the strain hardening in the stress−strain curve, up the draw ratio of about 7, where the sample breaks. The persistence of the neck up to $\lambda = 4$, prevented to obtain intermediate draw ratios in the range 1−4. Therefore, the first fiber of sample **1A** that we could analyze was characterized by a draw ratio of 4, and the maximum obtainable was $\lambda = 7$. At variance, sample **1B** homogeneously deforms, without neck formation, but, for comparison, also in this case we prepared fibers from $\lambda = 4$, up to $\lambda = 7$, which is the maximum obtainable draw ratio, at room temperature.

Here we discuss first the structure of the fibers obtained from sample **1B**, because it is easier to interprete.

In Figure 3 we show the X-ray fiber diffraction patterns of the samples with a draw ratio $\lambda = 4$ (**2B**), $\lambda = 5$ (**3B**), $\lambda = 6$ (**4B**), and $\lambda = 7$ (**5B**). We want to recall that the patterns were obtained by holding the fibers under tension. For comparison, in the figure we also show the pattern of the starting sample **1B**. In Table 1 all the reflections, the spacing and the corresponding 2ϑ (Cu) with the indices *hkl* for the helical and trans-planar forms are reported.

The pattern **2B**, relative to $\lambda = 4$, indicates that the sample, at this draw ratio, is already oriented, although not completely. On the equator we observe a polarized reflection, corresponding to the same diffraction angle as the starting sample. Therefore, it is the mesophase, orienting during the drawing: the orientation is clearly not completed, and the reflection, although quite sharp, is not yet completely concentrated on the equator. On the first layer, we observe a weak reflection corresponding to an identity period of 5.05 Å: it is the (021) reflection of the trans-planar form, that, although very weak, indicates the presence of this form orienting during drawing and getting more ordered. Very weak reflections both on the equator ($2\vartheta_{Cu} = 12.3°$) and on the first layer ($2\vartheta_{Cu} = 20.9°$) characteristic of the helical form are observable, too. They are due to the small fraction of the helical form present in the starting sample, which is orienting too.

Going to the successive draw ratio, the pattern is not substantially changed: the equatorial reflection of the mesophase results more concentrated, indicating a further orientation. Also the first layer reflection of the trans-planar form is more concentrated, although still weak. The very weak helical reflections have disappeared.

In the sample drawn at $\lambda = 6$ (**4B**) the equatorial reflection is split in two well polarized reflections, corresponding to the equatorial reflections of the crystalline form III. They are the (020) and (110) reflections, reported by Chatani.[8] On the equatorial line, also the very weak reflection (130) of the same structure appears. On the first layer there is only one reflection, the (021) of the trans-planar form, appearing still weak. In the sample drawn to $\lambda = 7$ (**5B**), the structure of form III is well developed, and besides the three reflections on the equator, two reflections on the first layer, corresponding to (021) and (111) planes of the Chatani form III, are now well observable. From these results we can conclude that drawing the mesophase, with the chains in trans-planar conformation, we obtain first the orientation of the mesophase and successively, at a draw ratio corresponding to 6, the transformation into the oriented crystalline form III, which appears well developed and oriented in the sample with draw ratio $\lambda = 7$. At $\lambda = 6$ and 7, no reflections of the helical form are visible.

In Figure 4 we show the X-ray fiber diffraction patterns of the fibers with a draw ratio $\lambda = 4$ (**2A**), $\lambda = 5$ (**3A**), $\lambda = 6$ (**4A**), and $\lambda = 7$ (**5A**), obtained from the starting sample **1A**, quenched for 1 min at 0 °C. We want to recall that, also in this case, the patterns were obtained by holding the fibers under tension. For comparison we report also the pattern of the starting sample **1A**. All the reflections, the spacing and the corresponding 2ϑ, with the indices *hkl* of the allowed forms are reported in Table 2.

First of all, we observe that the fiber drawn at $\lambda = 4$, after the neck propagated to the whole sample, is already quite well oriented, as in the previous case.

On the equator, the first strong spot corresponds to the (200) reflection of the helical form, present both in form I and in form II. The second spot, very strong, is

Table 1. Reflections Observed in the X-ray Fibers Diffraction Spectra of Sample B

sample	period along chain axis (Å)	2θ, deg (Cu)	distance (Å)	*I*	*hkl* (crystalline forms where the reflection is allowed)
2B (fiber $\lambda = 4$)					200 form I[a]
		12.32	7.18	vw	200 form I[b]
					200 form II
		16.0−18.0		vs	for the interpretation refer to the text
		29.47	3.03	vvw	130 form III
					111 form I[a]
	7.45	20.86	4.26	vw	121 form I[b]
					111 form II
	5.05	23.73	3.75	ms	021 form III
3B (fiber $\lambda = 5$)		16.0−18.0		vs	for the interpretation refer to the text
		29.47	3.03	vw	130 form III
	5.05	23.73	3.75	ms	021 form III
4B (fiber $\lambda = 6$)		15.87	5.58	vs	020 form III
		18.76	4.73	vs	110 form III
		29.47	3.03	ms	130 form III
	5.05	23.73	3.75	s	021 form III
5B (fiber $\lambda = 7$)		15.87	5.58	vs	020 form III
		18.76	4.73	vs	110 form III
		29.47	3.03	ms	130 form III
	5.05	23.73	3.75	s	021 form III
		25.78	3.46	ms	111 form III

[a] Form I orthorhombic unit cell with axes $a = 14.50$ Å, $b = 5.60$ Å, and $c = 7.45$ Å [b] Form I orthorhombic unit cell with axes $a = 14.50$ Å, $b = 11.20$ Å, and $c = 7.45$ Å

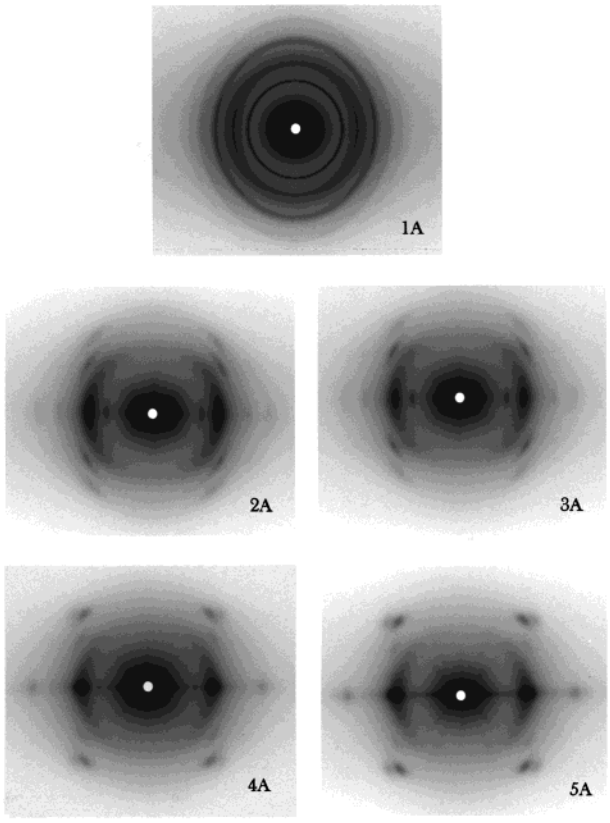

Figure 4. X-ray fiber diffraction patterns of the fibers with draw ratios $\lambda = 4$ (**2A**), $\lambda = 5$ (**3A**), $\lambda = 6$ (**4A**), and $\lambda = 7$ (**5A**), obtained from sample **1A**.

not easily interpretable: it could be either the (110) of the helical form II, or a superposition of the (020) or (010) reflection of the helical form I (ordered and disordered, respectively), and the oriented reflection of the trans-planar mesophase. It is worth recalling that in the starting **1A** sample there is a small fraction of trans-planar mesophase, as evidenced both by X-rays and infrared analysis, and more chains in trans-planar conformation are formed during the drawing process. The third spot, very weak, corresponds to the (400) reflection, common to both the helical form I and form II. On the *hk*1 layer we observe a strong reflection, corresponding to the identity period 7.45 Å: it could be indexed as (111) of the disordered form I, as (121) of the limit ordered form I with doubled *b* axis, or as (111) of form II. In any case it is a reflection of a helical form, either I or II. Another weak reflection, corresponding to an identity period of 5.05 Å, is distinguishable and must be indexed as a reflection (021) of the trans-planar form. In conclusion, the sample drawn at $\lambda = 4$ shows the prevalence of an oriented helical form together with a small fraction of oriented phase in trans-planar conformation, as resulting by the presence of the reflection with identity period 5.05 Å on the first layer. As for the helical form, it is not possible to discriminate between form I or form II: indeed the presence of the trans-planar reflection, corresponding to an identity period of 5.05 Å on the first layer, indicates the presence of the trans-planar form and suggests that the second strong reflection on the equator could be due to a superposition of the reflection of form I (either ordered or disordered) and that of the trans-planar mesophase. The same situation is observable for the sample drawn at $\lambda = 5$ (**3A**), very similar to the previous one.

At variance, in the sample drawn at $\lambda = 6$ (**4A**) the helical reflections, either the (200) on the equator, or the (121) on the first layer are very weak, almost indistinguishable, whereas the reflections of the trans-planar form are strong and well resolved. Indeed, the second spot on the equator now is split in two reflections, corresponding to the (020) and (110) reflections of the trans-planar form III, described by Chatani.[8] On

Table 2. Reflections Observed in the X-ray Fibers Diffraction Spectra of Sample A

sample	period along chain axis (Å)	2θ, deg (Cu)	distance (Å)	I	*hkl* (crystalline form where the reflection is allowed)
2A (fiber $\lambda = 4$)					200 form I[a]
		12.32	7.18	vs	200 form I[b]
					200 form II
		15.4−18.4		s	for the interpretation refer to the text
					400 form I[a]
		24.79	3.59	w	400 form I[b]
					400 form II
					111 form I[a]
	7.45	20.86	4.26	ms	121 form I[b]
					111 form II
	5.05	23.73	3.75	mw	021 form III
3A (fiber $\lambda = 5$)					200 form I[a]
		12.32	7.18	vs	200 form I[b]
					200 form II
		15.4−18.4		s	for the interpretation refer to the text
					400 form I[a]
		24.79	3.59	w	400 form I[b]
					400 form II
		29.47	3.03	vvw	130 form III
					111 form I[a]
	7.45	20.86	4.26	ms	121 form I[b]
					111 form II
	5.05	23.73	3.75	mw	021 form III
4A (fiber $\lambda = 6$)					200 form I[a]
		12.32	7.18	vw	200 form I[b]
					200 form II
		15.87	5.58	vs	020 form III
		18.76	4.73	vs	110 form III
		29.47	3.03	w	130 form III
					111 form I[a]
	7.45	20.86	4.26	w	121 form I[b]
					111 form II
	5.05	23.73	3.75	ms	021 form III
		25.78	3.46	w	111 form III
5A (fiber $\lambda = 7$)		15.87	5.58	vs	020 form III
		18.76	4.73	vs	110 form III
		29.47	3.03	mw	130 form III
					111 form I[a]
	7.45	20.86	4.26	vvw	121 form I[b]
					111 form II
	5.05	23.73	3.75	s	021 form III
		25.78	3.46	ms	111 form III

[a] Form I orthorhombic unit cell with axes $a = 14.50$ Å, $b = 5.60$ Å, and $c = 7.45$ Å [b] Form I orthorhombic unit cell with axes $a = 14.50$ Å, $b = 11.20$ Å, and $c = 7.45$ Å

the first layer the reflection (021) corresponding to the identity period of 5.05 Å (trans-planar form III) is now much stronger than that of 7.45 Å. Therefore, at this draw ratio we observe the appearance of the crystalline trans-planar form III, although not yet completely ordered.

In the sample drawn at $\lambda = 7$ the reflections of the crystalline form III are very intense, and only a very weak reflection of the helical form is still present on the first layer.

Therefore, by drawing sample **1A**, which crystallized in a disordered form I, containing also a fraction of mesophase in trans-planar conformation, we obtained, for the first draw ratio after the neck propagation, an oriented helical form, and a small fraction of oriented trans-planar form, not yet corresponding to the crystalline form III. Only at higher draw ratios of $\lambda = 6$ and $\lambda = 7$ did we obtain the oriented crystalline form III.

In Figure 5 we show the FTIR spectra of the fibers drawn from sample **1B**. In all the samples the trans-planar bands, appearing at 831, 963, and 1132 cm^{-1}, are present and well developed as well as they were in the starting sample **1B** (see Figure 2). It is interesting to note that the trans-planar band at 831 cm^{-1}, is split in two bands when the crystalline form III is formed. Considering now the helical bands, we observe that the 810 and the 1005 cm^{-1} bands are completely absent, whereas the 977 cm^{-1} band decreases going from sample **2B** ($\lambda = 4$) to sample **5B** ($\lambda = 7$), where it appears only as a shoulder.

In Figure 6 we show the FTIR spectra of the fibers drawn from sample **1A**. As shown before (Figure 2) in

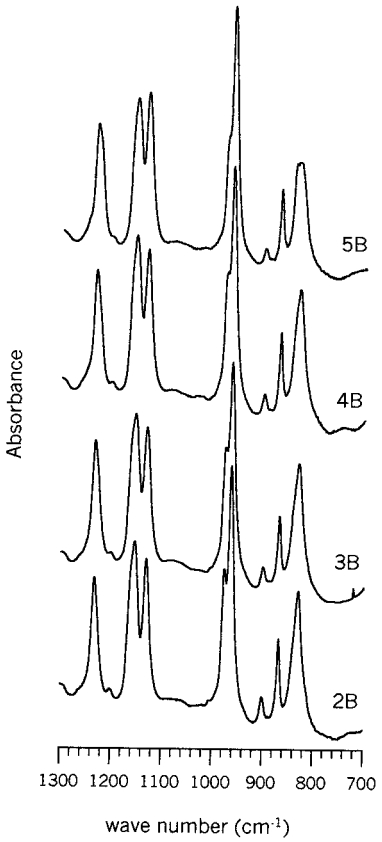

Figure 5. FTIR spectra in absorbance (1300−700 cm^{-1}) of the fibers drawn from sample **1B**.

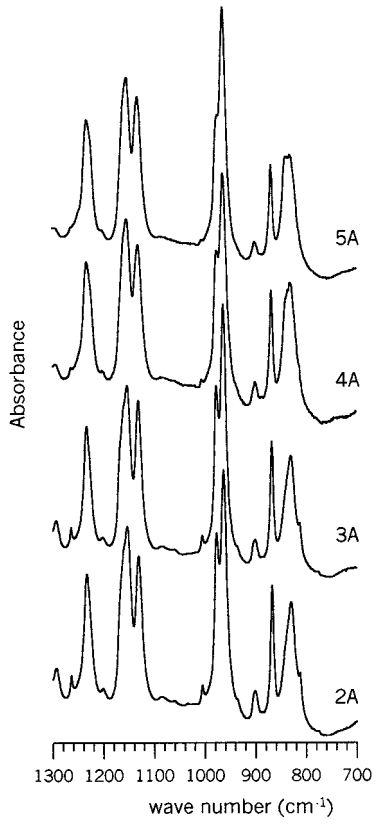

Figure 6. FTIR spectra in absorbance (1300−700 cm^{-1}) of the fibers drawn from sample **1A**.

the starting **1A** sample the helical bands were present and very intense, being this sample in the helical form I. We can observe that in the sample drawn at $\lambda = 4$ (**2A**), the helical bands at 810, 868, 977, and 1005 cm^{-1} are still present, although of lower intensity than in sample **1A**. They are strongly reduced or disappear in the samples drawn at $\lambda = 6$ (**4A**) and $\lambda = 7$ (**5A**). At variance, all the trans-planar bands increased very much respect to the starting sample. Also in this case the trans-planar band at 831 cm^{-1} is split when the crystalline form III appears. Indeed, the FTIR spectra of samples **5A** and **5B** are very similar, as the X-ray patterns.

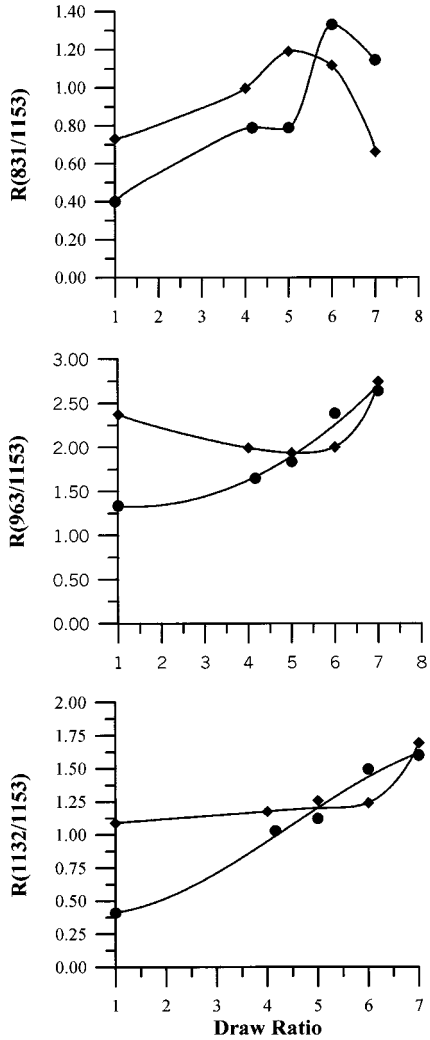

Figure 7. The ratio *R* for the trans-planar bands at 831, 963, and 1132 cm^{-1} as a function of the draw ratio for the fibers drawn from sample **1A** (●) and sample **1B** (♦).

To follow the development of the trans-planar infrared bands in the two different series of fibers, we normalized the absorbance of these bands with the absorbance of the band at 1153 cm^{-1}, which is independent of the conformation,[28] obtaining the ratio

$$R = \text{absorbance}_{(\text{trans-planar band})}/\text{absorbance}_{(1153\ \text{cm}^{-1})}$$

The band at 1153 cm^{-1} which overlaps with other vibrational modes, was decomposed in the different components, as showed before in the Experimental Section.

In Figure 7 we report the ratio *R* for the three trans-planar bands at 831, 963, and 1132 cm^{-1}, as a function of the draw ratio. For the fibers drawn from sample **1A** we can observe a strong increase of the *R* parameter going from the starting sample to the first fiber, at $\lambda =$

Table 3. Reflections Observed in the X-ray Diffraction Spectra of Relaxed Fibers

sample	period along chain axis (Å)	2θ, deg (Cu)	distance (Å)	I	*hkl* (crystalline form where the reflection is allowed)
1C (relaxed fiber $\lambda = 3.8$)					200 form I[a]
		12.32	7.18	vs	200 form I[b]
					200 form II
		15.7−18.2		s	for the interpretation refer to the text
					400 form I[a]
		24.79	3.59	ms	400 form I[b]
					400 form II
					111 form I[a]
	7.45	20.86	4.26	s	121 form I[b]
					111 form II
		27.38	3.26	mw	311 form I[a]
					321 form I[b]
	5.05	23.73	3.75	mw	021 form III
2C (relaxed fiber $\lambda = 4$)		∼17.0	5.21	s	trans-planar mesophase
					111 form I[a]
	7.45	20.86	4.26	vvw	121 form I[b]
					111 form II
	5.05	23.73	3.75	m	021 form III

[a] Form I orthorhombic unit cell with axes $a = 14.50$ Å, $b = 5.60$ Å, and $c = 7.45$ Å [b] Form I orthorhombic unit cell with axes $a = 14.50$ Å, $b = 11.20$ Å, and $c = 7.45$ Å.

4, and then a further increase up to $\lambda = 7$. Only the band at 831 cm^{-1} shows a decrease at $\lambda = 7$, but it is worth recalling that this band splits in two bands when the crystalline form III is obtained, and this explains its decrease for draw ratio 7.

In the case of sample **1B**, which already had the chains in trans-planar conformation, we observe an increase for the band at 831 cm^{-1}, an almost constant value for the band at 1132 cm^{-1}, and an initial decrease for the band at 963 cm^{-1}, followed again by an increase. We suggest that this band contains a strong contribution of the trans-planar mesophase, and it decreases at the beginning, due to a decrease of mesophase. As before, the R parameter for the band at 831 cm^{-1} decreases at $\lambda = 7$, when the crystalline form III is obtained.

The interesting observation is that the two series of samples reach for $\lambda = 7$ almost the same value of the R parameters relative to the 963 and 1132 cm^{-1}, as well as they show very similar X-ray diffraction patterns.

Relaxed Fibers. After the release of the applied tension, the fibers drawn at $\lambda = 6$ both from sample **1A** and **1B** strongly contract, reaching $\lambda = 3.8$ and 4.0, respectively. They were analyzed by X-rays (Table 3) and infrared spectra, to follow the conformational transitions and to observe if they behave in a similar manner.

In Figure 8 we report the X-ray diffraction patterns of the fibers obtained from sample **4A** (sample **1C**) and from sample **4B** (sample **2C**). In the first case we can observe a partial transition from the trans-planar form III into the helical form. The reflections of the oriented helical form are present on the equator, as well as in the first layer. A very weak reflection of the trans-planar form is still observable on the first layer. The residual presence of chains in trans-planar conformation, as suggested by this reflection, again makes it difficult to interpret the second spot on the equator: it could be the (110) reflection of the helical form II or a superposition of the (020) reflection of the helical form I and a reflection of the trans-planar mesophase, formed on disordering form III.

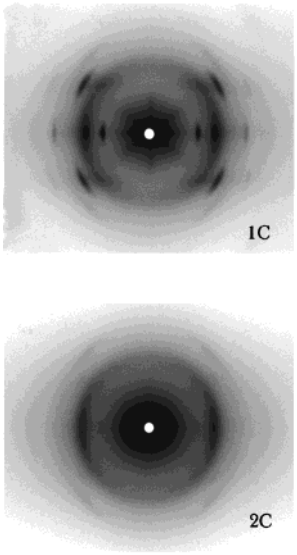

Figure 8. X-ray diffraction patterns of the fibers after releasing the tension of sample **4A** (**1C**) and sample **4B** (**2C**).

The pattern of sample **2C** is clearer, being present the polarized reflection of the trans-planar mesophase on the equator, and the reflection corresponding to the trans-planar form on the first layer, too. In this case undoubtedly the crystalline form III transformed in the oriented mesophase, upon releasing the tension. These results are confirmed by the FTIR spectra shown in Figure 9.

The helical bands, which were completely absent or strongly reduced in sample **4A** (see Figure 6), increased in the released sample **1C**. At variance sample **2C** we do not observe the appearance of the helical bands at 810 and 1005 cm-1: only the band at 973 cm^{-1} is slightly increased, and the spectrum is very similar to that of the sample **2B** ($\lambda = 4$).

This result shows that, despite the similarity of the fibers at $\lambda = 6$ under tension, when released they transform into different forms with a memory of the initial structure: the sample coming from the form I

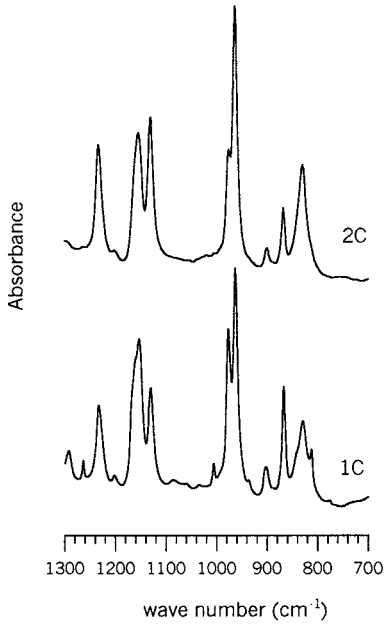

Figure 9. FTIR spectra in absorbance (1300−700 cm^{-1}) of the fibers **1C** and **2C**.

and the sample coming from the mesophase, upon releasing the tension, undergo different transformations, going toward the oriented helical form the first, and the oriented trans-planar mesophase the second. Both show a large shrinkage and an elastic behavior.

Work is in progress to understand the reasons of the strong shrinkage and the nature of the elastic behavior.

Acknowledgment. This work was supported by Ministero dell'Università e della Ricerca Scientifica e Tecnologica (PRIN 1998 titled "Stereoselective Polymerization: New Catalist and New Polymeric Materials")

References and Notes

(1) Ewen, J. A.; Jones, J. A.; Razavi, A.; Ferrara, J. D. *J. Am. Chem. Soc.* **1988**, *110*, 6255.
(2) Longo, P.; Proto, A.; Grassi, A.; Ammendola, P. *Macromolecules* **1992**, *24*, 462.
(3) Grisi, F.; Longo, P.; Zambelli, A.; Ewen, J. A. *J. Mol. Catal. A: Chem.* **1999**, *140*, 225.
(4) Lotz, B.; Lovinger, A. J.; Cais, R. E. *Macromolecules* **1988**, *21*, 2375.
(5) Lovinger A. J.; Lotz, B.; Cais, R. E. *Polymer* **1990**, *31*, 2253.
(6) Lovinger, A. J.; Davis, D. D.; Lotz, B. *Macromolecules* **1991,** *24*, 552.
(7) Lovinger, A. J.; Lotz, B.; Davis, D. D.; Padden, F. J. *Macromolecules* **1993,** *26*, 3494.
(8) Chatani, Y.; Maruyama, H.; Noguchi, K.; Asanuma, T.; Shiomura, T. *J Polym. Sci., Part C* **1990**, *28*, 393.
(9) Chatani, Y.; Maruyama, H.; Asanuma, T.; Shiomura, T. J. *J. Polym. Sci., Polym. Phys. Ed.* **1991,** *29*, 1649.
(10) De Rosa, C.; Corradini, P. *Macromolecules* **1993**, *26*, 5711.
(11) Auriemma, F.; Lewis, R. H.; Spiess, H. W.; De Rosa, C. *Macromol. Chem. Phys.* **1995**, *196*, 4011.
(12) De Rosa, C.; Auriemma, F.; Corradini, P. *Macromol. Chem.* **1996**, *29*, 7452.
(13) De Rosa, C.; Auriemma, F.; Vinti, V. *Macromolecules* **1997,** *30***,** 4137.
(14) De Rosa, C.; Auriemma, F.; Vinti, V. *Macromolecules* **1998,** *31***,** 9253.
(15) Lacks, D. J. *Macromolecules* **1996,** *29***,** 1849.
(16) Palmo, K.; Krimm, S. *Macromolecules* **1996**, *29***,** 8549.
(17) Uehara, H.; Yamazaki, Y.; Kanamoto, T. *Polymer* **1996**, *37*, 57.
(18) Loos, J.; Buhk, M.; Petermann, J.; Zoumis, K.; Kaminsky, W. *Polymer* **1996,** *37*, 387.
(19) Loos, J.; Petermann, J.; Waldofner, A. *Colloid Polym. Sci.* **1997**, *275*, 1088.
(20) Nakaoki, T.; Ohira, Y.; Hayashi, H. *Macromolecules* **1998**, *31*, 2705.
(21) Vittoria, V.; Guadagno, L.; Comotti, A.; Simonutti, R.; Auriemma, F.; De Rosa, C. *Macromolecules*, in press.
(22) Loos, J.; Huckert, A.; Petermann, J. *Colloid Polym. Sci.* **1996,** *274*, 1006.
(23) D'Aniello, C.; Guadagno, L.; Vittoria, V. Submitted for publication.
(24) Guadagno, L.; Fontanella, C.; Vittoria, V.; Longo, P. *J. Polym. Sci., Part C* **1999,** *37*, 173.
(25) Corradini, P.; Natta, G.; Ganis, P.; Temussi**,** P. *J. Polym. Sci. C* **1967** *16*, 2477.
(26) Natta, G.; Corradini, P.; Ganis, P. *Makromol. Chem.* **1960, 39,** 238.
(27) Guadagno, L.; D'Arienzo, L.; Vittoria, V. *Macromol. Chem. Phys.* 2000 *201*, 246.
(28) Guadagno, L.; D'Aniello, C. Unpublished results.

MA0005973